Spin-Density Oscillations in Ferromagnetic Alloys. I. "Localized" Solute Atoms: Al, Si, Mn, V, and Cr in Fe

MARY BETH STEARNS
Scientific Laboratory, Ford Motor Company, Dearborn, Michigan
(Received 30 November 1965)

The internal magnetic fields and isomer shifts of Fe^{57} nuclei in a number of iron-rich bcc binary alloy systems were measured by the Mössbauer technique. The added solute atoms Al, Si, Mn, Cr, or V give structure to the individual lines of the spectra indicating that their effects are quite localized. These line shapes were analyzed by a computer program which interpreted them in terms of the effects of the solute atoms in the first five neighbor shells. It appears justifiable to attribute the observed hyperfine-field shifts in the FeAl series to the spatial variation of the spin polarization of the 4*s* conduction electrons around an Fe atom in pure iron. The observed 4*s* spin-polarization variation with distance had oscillations with a $k_F \simeq (1.0\text{–}1.2)\times 10^8$ cm^{-1} corresponding to 0.4–0.6 electrons/atom in the 4*s* conduction band. These oscillations are compared with those obtained by recent improved calculations of the indirect exchange polarization which take into account the full k dependence of the conduction-electron wave functions. For all the alloy series reported here, internal field shifts at the first and second nearest neighbors decreased the internal field. This indicates that the 4*s* electrons produce an antiferromagnetic contribution to the magnetic coupling in iron. The average internal field of each alloy was also obtained, and for all the alloy series described here this quantity decreases more rapidly than the moment per Fe atom as a function of solute-atom concentration. The isomer shifts due to solute atoms in the first three neighbor shells are also reported.

I. INTRODUCTION

MÖSSBAUER spectra of Fe^{57} in any material give information about the magnitude and polarization of the wave functions of the *s* electrons at the Fe^{57} nuclei. These charge and spin densities in turn depend on the environment surrounding an Fe atom. In particular it has been found[1,2] that Mössbauer spectra can be analyzed to give detailed information about the magnetic environment of an Fe atom in ferromagnetic alloys and we report here the results of studies made on bcc Fe-rich random binary alloys (>85% Fe). All solute atoms studied thus far yield Mössbauer spectra which can be characterized by two behavior patterns. The first type of solute atoms give spectra that closely resemble that of pure Fe: i.e., six symmetrical structureless lines which are somewhat broadened, depending on the concentration of the solute atoms. Typical of solute atoms which fall into this category are Co, Ni,[3] Au, and Pt which we have studied, and Pd[4] and Rh (<10 at.%)[5] as reported by others. The magnetic effects of the solute atoms are either mainly nonlocalized or they may be localized but produce too small a change in the internal field of nearby iron atoms to be resolved by the Mössbauer technique. [Because of the natural linewidth of the Fe line, this technique has a poor inherent resolution (~16 kG) compared to NMR experiments. Recent spin-echo experiments[6] show some structure in the spectra of alloys with Co and Ni solute atoms.] Alloys of these solute atoms will not be discussed here but are to be reported in a subsequent paper. The second type of solute atoms give spectra with a gross six line spectra but the individual lines, especially the outer two, show much structure indicating that the solute-atom effects of this group behave as if they are well localized. We have studied and herein report on the bcc alloy systems of Al, Si, Mn, V, and Cr solute atoms. Their spectra can be analyzed to yield detailed information regarding variations of internal fields and isomer shifts of the Fe atoms as a function of their atomic positions relative to the impurity atoms. In the present work we analyze the shape of the outer lines to obtain the effect on the spin density at an Fe^{57} nucleus due to a solute atom in the first three to five nearest-neighbor (nn) shells.

Recently many groups have been attempting similar measurements of the internal magnetic fields using NMR techniques. These techniques have an energy resolution which is about a factor of 7 (for spin echo) to 30 (for frequency-swept super-regenerative oscillator) times better than that possible in Mössbauer experiments using Fe^{57}. Many of the same alloys have now been looked at by the two techniques.[6] The NMR results are in qualitative agreement with the work reported here although there is some disagreement in the details. These results are being prepared for publication.

The observed variation in internal fields may be interpreted as due to the oscillations in the spin density of the 4*s* conduction electrons. (The reader should note that 4*s*-3*d* mixing occurs in the transition metals and causes significant changes, for example in the topology

[1] M. B. Stearns, (a) Phys. Rev. **129**, 1136 (1963); (b) J. Appl. Phys. **25**, 1095 (1964); (c) M. B. Stearns and S. S. Wilson, Phys. Rev. Letters **13**, 313 (1964); M. B. Stearns, J. Appl. Phys. **36**, 913 (1965).

[2] G. K. Wertheim, V. Jaccarino, J. H. Wernick, and D. N. E. Buchanan, Phys. Rev. Letters **12**, 24 (1964).

[3] Many of these systems have been studied by C. E. Johnson, M. S. Radout, and T. E. Cranshaw, Proc. Phys. Soc. (London) **81**, 1079 (1963). They report an estimated average internal field.

[4] P. P. Craig, B. Mozer, and R. Segman, Phys. Rev. Letters **14** 895 (1965).

[5] G. Shirane, C. W. Chen, P. A. Flinn, and R. Nathans, Phys. Rev. **131**, 183 (1963).

[6] M. Rubinstein, G. H. Stauss, and M. B. Stearns, J. Appl. Phys. Suppl. **37**, 1334 (1966).

of the Fermi surface. However, the experimental phenomena studied here should arise primarily from the 4*s* components of wave functions and depend, moreover, on the perturbability of all the states in the zone—not selectively on the small fraction of states for which 4*s*-3*d* mixing cannot be ignored. Consequently we have reason to hope that the sharp distinction between 4*s* and 3*d* bands which we adopt here for the sake of clarity and simplicity is adequate.) The measured form of the polarization can be compared to theories[7] which attribute the origin of ferromagnetism to the indirect exchange interaction of the coupling of the spins of magnetic ions via the conduction electrons. This comparison with theory and some recent versions[8,9] with corrections to the free-electron approximation used in the earlier theory is given in Sec. VI. The variations of the isomer shift with alloying is also reported.

II. EXPERIMENTAL PROCEDURE

A typical Mössbauer setup was used. The motion system has been described in earlier work[10] and consists of a vibrator driven to produce a linear change in velocity with a frequency of about one cycle/sec. The motion system has been modified from that of Ref. 10 and now contains two additional corrections for inertia and friction. These corrections reduce the error signal and thus improve the linearity of the motion. The error signal is at most 0.2% of the peak-to-peak voltage. The data were taken with a maximum velocity of about 7 mm/sec so the broadening due to the motion system was at most 0.03 mm/sec. The modulation for the pulses into the multichannel analyzer was obtained directly from a velocity pickup coil. A second source of broadening is the finite collimation of the γ rays. This causes the γ rays which are not traveling in the direction of the motion to be Doppler shifted with a lesser velocity than that of the motion. For the geometry used this broadening was about 8×10^{-3} times the velocity of motion, which corresponds to a broadening of the inner lines of the spectrum of the Armco Fe absorber of about 0.01 mm/sec. A third source of broadening is that due to finite absorber thickness.[11] For a 1-mil-thick absorber such as we used, the broadening of the inner Fe lines due to this effect is about 0.01 mm/sec. The sum of these three effects agrees with the observed broadening of these inner lines, whose typical widths was 25% greater than the natural linewidth (0.19 mm/sec).

The source was Co^{57} diffused into a Pt or Pd foil. These matrices apparently give a source having the natural linewidth.

The alloys were all prepared in an induction furnace by melting the pure elements ($\geq$99.9%) in either a vacuum or argon atmosphere and then rolling the ingots to 3–5 mils. They were then heat treated in a manner which randomized them as much as possible and finally etched down to $\frac{1}{2}$- to 1-mil thickness. Many of the alloy systems were difficult to randomize completely and were quite sensitive to heat treatment. The systems studied were the bcc alloys of Fe with Al, Si, Mn, V, and Cr. The Al alloys were easily disordered by heating in an argon atmosphere at 800–900°C for 2 to 3 h and then quenching to room temperature. However, care had to be taken to prevent the alloys from losing Al in the heat treatment. This was achieved by heat treating samples thick enough that when etched down to the final thickness the foils were of the original composition. Alloys of Si, V, and Cr showed signs of order at all compositions and all quench rates. The latter were heat treated in two ways: (1) encapsulated in an argon atmosphere and brought to 800–900°C, kept there for at least 2 h, and then quenched at different rates to room temperature and (2) brought to 900°C in a hydrogen atmosphere and held there for at least 2 h and then dropped directly into an oil bath which was at room temperature. For none of these alloys was there a drastic change in spectra as long as the alloys were cooled reasonably rapidly, the structure however did decrease slightly the faster the quench rate and it appeared that procedure (2) which had the most rapid quench rate produced spectra that most closely resembled true random alloys. The Mn alloys of Mn content <3 at.% (throughout this paper all compositions will be given in atomic percent) behaved as if well disordered for the usual heat treatment above, (1). The higher ($\geq$4.7) percent Mn alloys behaved in the following manner: Here moderate or slow cooling produced a large paramagnetic peak near zero velocity. It was necessary to quench rapidly to avoid this nonmagnetic phase. The quick-quenched Mn alloys showed spectra very typical of complete disorder. This behavior is apparently typical of alloys with phase diagrams similar to that of the Fe-Mn system.

We tested the alloys for homogeneity by checking many samples with an electron probe in steps of about 3 μ. The results indicated that the alloys used were of uniform composition and of the same chemical composition as before heat treatment. Chemical analysis was made in the 3–5-mil rolled stage of all the samples. In all cases these compared accurately with the chemical analysis on the bulk ingots from which the material for rolled samples was taken. Also in some cases we chemically analyzed the final heat-treated material and this was also found to be of the same chemical composition as before heat treatment.

The data were taken at room temperature with a counting rate of about 500 cps by alternating the alloys

[7] M. A. Ruderman and C. Kittel, Phys. Rev. **96**, 99 (1954); T. Kasuya, Progr. Theoret. Phys. (Kyoto) **16**, 45 (1956); K. Yosida, Phys. Rev. **106**, 893 (1957); called RKKY calculations.
[8] T. A. Kaplan, Phys. Rev. Letters **14**, 499 (1965).
[9] R. E. Watson and A. J. Freeman, Phys. Rev. Letters **14**, 695 (1965).
[10] D. Rubin, Rev. Sci. Instr. **33**, 1358 (1962).
[11] See, e.g., D. A. Shirley, M. Kaplan, and P. Axel, Phys. Rev. **123**, 816 (1961).

with Armco Fe calibration runs, i.e., an Fe run of about 8 h, two alloy runs of 24 h each, again an Fe run, etc. Only those data were used for which the preceding and following Fe runs indicated that the apparatus was operating in optimum fashion. The criteria for a good Fe run are discussed in the next section.

III. EXPERIMENTAL ANALYSIS

The Fe data are analyzed as follows. The computer is fed the raw data and fits the complete spectrum with a curve made up of the sum of modified Lorentzians and a continuous background as expressed by

$$B+Ax-\sum_{i=1}^{6}\frac{h_i}{[|x-x_i|/\Gamma_i]^{n_i}+1}, \tag{1}$$

where $B+Ax$ is the background in channel x, and Ax represents the nonlinearities in the system, mainly the nonlinearities in the analog-to-digital converter of the multichannel analyzer. (Most of the data were taken with a blocking circuit into the analyzer which eliminated a slope due to the dead time of the analyzer.) h_i is the height of the line located at x_i, Γ_i, is the full width at half-maximum, and n_i is a parameter which would be 2 for a true Lorentzian but, because of many effects (finite thickness, broadening due to motion and collimation, etc), it usually has a value between 2.0 and 2.5. B, A, and six sets of values of x_i, Γ_i, h_i, and n_i are obtained by minimizing the sum of the squares of the difference between the computed and experimental points (mean-square deviation, MSD). Besides the parameters already mentioned the computer also calculated the relative areas of each line and isomer shift of the outer two sets of peaks. The differential nonlinearity (DNL) of the multichannel pulse-height analyzer (Nuclear Data Corporation) manifests itself by increasing the root-mean-square deviation (R) of the calculated and observed spectra over the standard deviation ($S=\sqrt{N}$) as calculated straightforwardly from the number of counts N in the measurement. Dividing R and S by the total number of counts N and multiplying by 100 we obtain relative percentage quantities which are more convenient to use, i.e., $r=R/N\times 100$, $s=S/N\times 100$. Then r is given by

$$r^2=s^2+d^2, \tag{2}$$

where d^2 is the average of the squares of the percentage differential nonlinearity of the analyzer. Figure 1 shows a graph of r versus s for some of the Fe calibration runs. The curve shown is of the form of Eq. (2) with $d\sim 0.2\%$. Actually the DNL varies greatly from channel to channel, some channels of our analyzer had differential nonlinearities as high as 0.7%. Our analyzer had been selected to have a small value of d; for most commercially available analyzers d is probably about twice as great as for our analyzer. The DNL of a multichannel analyzer is not random from channel to channel but behaves in a regular fashion which depends upon the construction of the analyzer. We have measured this behavior in our analyzer and find that besides regular variation in magnitude, the sign of the DNL alternates from channel to channel. A good Fe run was considered to be one whose rms deviation fell close to the curve of Fig. 1.

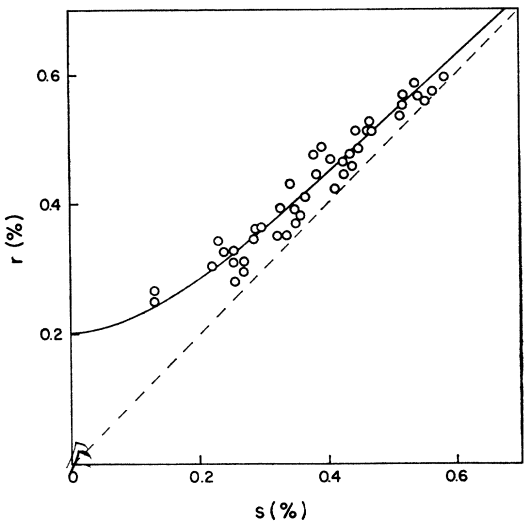

FIG. 1. Variation of the relative percentage rms deviation r with the relative percentage standard deviation s for the Fe calibration runs. The curve shown is a plot of $r^2=s^2+(0.2)^2$. The parabolic behavior arises from the differential nonlinearity of the multichannel pulse-height analyzer as discussed in the text.

In analyzing the data of the alloys we considered only the outer peaks (except where otherwise stated). In this case we corrected for the DNL by averaging over adjacent channels. The number of counts taken in each channel for an alloy run was such that the statistical error was $\leq d(0.2\%)$. Care was taken to use enough channels such that the outer lines covered a sufficient number of channels so that no detail was lost by the pairwise averaging. The averaging was made by considering both possible types of pairing, i.e., for a given channel n, we consider both possibilities n and $(n+1)$ and also n with $(n-1)$. Throughout the discussion of the analysis by the experiments curve, we mean such averaged experimental data.

We will give a somewhat historical account of the development of our analysis of the Mössbauer spectra in order to clearly give evidence that we need to consider at least three neighbor shells to get a good fit to the data.

$N1$ Analysis

Originally we analyzed the alloys by considering only the nearest neighbors ($N1$).[1(a),(b)] For this analysis we calculated the probabilities for each alloy of each of the possible nine (8 nn) configurations around an Fe atom. With these weighting factors the computer then calculated a curve by summing over those configurations

which had a probability greater than 0.04. The positions, width, and shape of the individual contributions was varied to obtain a minimum in the MSD. The width and shape were allowed to vary from alloy to alloy but kept the same for all components of a given alloy. The line shape was given by a function similar to the third term of Eq. (1). This analysis gave results whose systematic behavior indicated that second nearest neighbors ($N2$) should be considered. Specifically this behavior was (1) the internal field for an Fe atom with a given number of nearest neighbors decreased with an increase in solute atom concentration [see Fig. 3 of Ref. 1(b)] and (2) the widths of the individual components increased with solute atom concentration.

One very salient result of this $N1$ analysis was that the shifts due to each neighbor were additive; that is, for a given composition, n nearest-neighbor solute atoms produced n times the effect of one nearest-neighbor solute atom. See Fig. 4 of Ref. 1(a) and Fig. 2 of Ref. 1(b). Additivity had also been observed to be strongly evident in the *ordered* alloys of the FeSi[1(a)] and FeAl[1(b)] series.

$N2$ Analysis

We therefore proceeded to analyze the data considering first and second neighbors. Now instead of nine possible occupational configurations for each Fe atom we have 9×7 possibilities (6 nnn). Here we had the computer calculate the probability for each occupational configuration having a probability of greater than 0.01. We again assumed a shape similar to the third term of (1) but no additivity was assumed. The results gave lower MSD than the $N1$ analysis but again discrepancies similar to those observed in the $N1$ analysis occurred. The discrepancies were in a direction which indicated that the third neighbor increases the internal field in the FeSi and FeAl alloys. Again additivity was strongly evident in the $N2$ analysis for all alloy systems. The fact that additivity was so prevalent in all the analyses gives evidence that these solute atoms really act independently and are well localized.

For further analysis of the data we then assumed that additivity occurs and for a given alloy we consider as many nearest-neighbor shells as have sensitivity in reducing the MSD in the analysis; in the best cases this is five.

$N3$–$N5$ Analysis

The first five neighbors occupation numbers for a bcc lattice are 8, 6, 12, 24, 8. Thus if we consider the five nearest shells there are $9\times7\times13\times25\times9$ possible occupational configurations for the Fe atoms. For a given alloy each site has a fixed probability to be occupied by a solute atom (or an Fe atom). The computer calculates the probabilities of all the possible occupational configurations surrounding an Fe atom and retains all terms which are needed to make a total probability of 0.99. Since additivity is assumed in this analysis, the parameters to be determined correspond to the internal field shifts (ΔH_n) due to a single solute atom in the nth shell. A line shape of the form given by the third term of Eq. (1) is used; however, now Γ and n are no longer parameters, but are determined from the Armco Fe calibration runs. In the course of the development of the analysis, Γ and n were varied to determine how sensitive the final internal field shifts were to their assumed values. It was found that indeed the width and power obtained from the Armco Fe runs gave the minimum MSD and that the final ΔH_n's were quite insensitive to reasonable changes in Γ and n. If we consider five shells the shift of a given occupational configuration from that of the pure Fe position is thus given by

$$\Delta H=\sum_{n=1}^{5} m_n\Delta H_n, \tag{3}$$

where m_n is the number of solute atoms in a given nth-neighbor shell and ΔH_n is the internal-field shift due to the nth shell. At present we use a series of three computer programs to obtain and check the values of the ΔH_n's.

The first computer program (PI) scans large ranges of the ΔH_n's to obtain first estimates of the internal-field shifts for the first three neighbor shells. For ΔH_3 in a fixed range of values, ΔH_1 and ΔH_2 are varied over a large range of values (e.g., for the 5.1% FeAl alloy ΔH_1 for the $-v$ curve is about -6.8 channels and ΔH_2 is -3.5 channels, PI typically would scan ΔH_1 from -3.0 to -8.0 and ΔH_2 from -2.0 to -7.0 while ΔH_3 was varied from -3.0 to $+3.0$). The results are printed out in the form of an error contour map and the areas within 10% of the minimum MSD are then examined in greater detail with a grid of a tenth of a channel. In general the experimental apparatus is such that the over-all stability is to about 0.1–0.2 channels over a series of runs. These error contour plots are similar in form to those of PIII which are shown in Fig. 4.

Having obtained a first estimate of ΔH_1, ΔH_2, and ΔH_3 we then go to a second program (PII) which can vary up to nine ΔH_n's independently. Starting with the values obtained in PI we vary ΔH_1, ΔH_2, ΔH_3 over suitable ranges while also varying ΔH_4 over a large range. After obtaining a good value for ΔH_4, we then scan ΔH_5 while also varying $\Delta H_1\cdots\Delta H_4$ over suitable ranges, etc. We found that the best criteria we could use to estimate the significance of each successive neighbor shell were indicated by the minimum MSD of each analysis as we included more neighbor shells. Thus PII is also used to obtain the minimum MSD for analyses considering progressively more neighbor shells. For example, in Table I we quote ratios of the MSD for the successive analysis of the FeAl alloys, i.e., $N1/N2$ is the ratio of the MSD of an analysis considering only $N1$ with that of a $N2$ analysis, etc. We

TABLE I. Ratio of minimum mean-square deviation for successive analysis of FeAl alloys.

	$N1/N2$		$N2/N3$		$N3/N5$	
At. % Al	$+v$	$-v$	$+v$	$-v$	$+v$	$-v$
1.95	8.0	10.3	3.4	2.1	1.01	1.04
3.8	4.3	11.5	12.7	1.8	1.05	1.1
5.1	9.1	11.3	8.7	5.2	1.07	1.02
10.6	18.4	29.7	2.4	6.5		
13.2	53.5	15.2	1.4	1.4		
15.2	44.7	70.6	3.4	2.5		

see that for all the alloy systems studied, the values of ΔH_4 and ΔH_5 are small, so only for the most favorable data do we have much sensitivity to them. Also since for a bcc lattice the fourth and fifth neighbors are very close in distance, it was observed that in a $N4$ analysis the ΔH_4 obtained assumed a value intermediate to ΔH_4 and ΔH_5 thus anticipating the value of ΔH_5. Thus the decrease in the MSD in adding the fifth shell to an $N4$ analysis is small. It is clear that the analysis containing five shells gives a better picture of the internal field shifts than the $N4$ analysis. For these reasons we omit $N3/N4$ and give the ratio of MSD for a $N3$ analysis

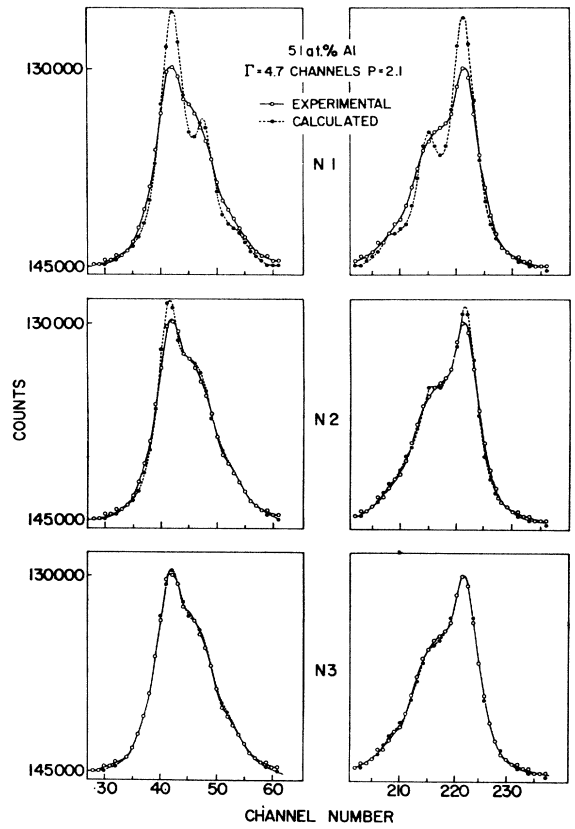

FIG. 2. Comparison of experimental and calculated curves obtained by considering progressively more neighbor shells in computer program II. The width Γ and power P were obtained from the Fe calibration runs. Where the experimental and calculated points are the same, only the former are shown.

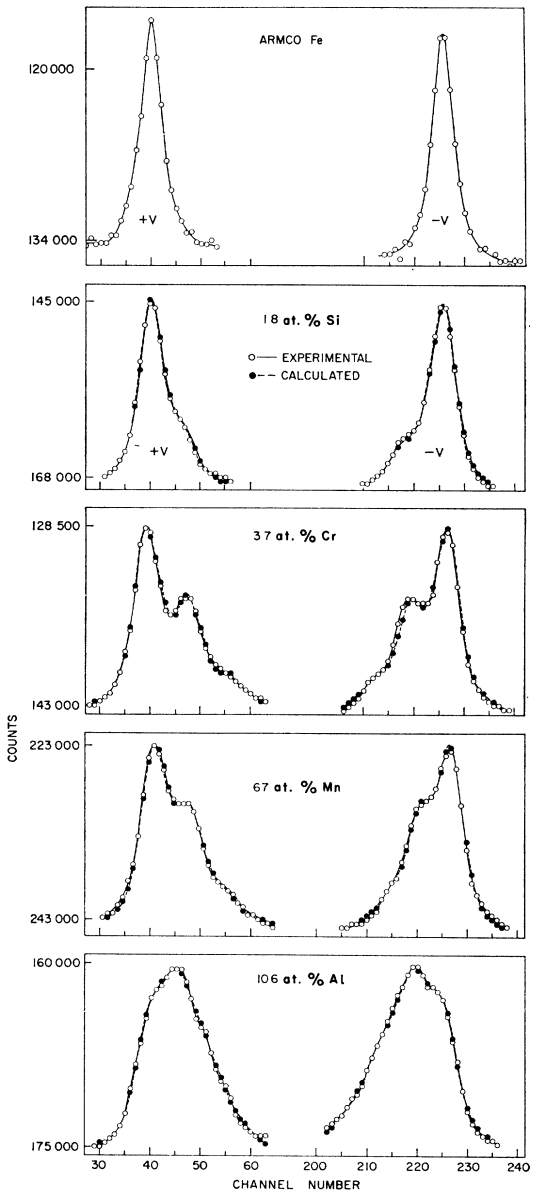

FIG. 3. Some typical outer lines showing the variation of line shapes and their computer analyzed fits for several of the alloys. Where the experimental and calculated points are the same, only the former are shown.

compared to the $N5$ analysis. We see from Table I that ΔH_1, ΔH_2, and ΔH_3 of the FeAl system are determined with good sensitivity and that ΔH_4 and ΔH_5 are strongly required to be small and so naturally we have less sensitivity to them. Figure 2 shows some typical comparisons of calculated and experimental curves for the various successive analyses. We see that the fit obtained with an $N3$ analysis is much better than those obtained with either an $N1$ or $N2$ analysis. Some typical fits obtained with an $N5$ analysis are shown in Fig. 3.

After determining the best ΔH_n's with PII we use a third program (PIII) whose purpose is to check that

TABLE II. Relative percent hyperfine-field shifts and average field for the FeAl series.

At. % Al	H_1	H_2	H_3	H_4	H_5	H_0	$\bar{H}_{\text{int}}$
1.95	−7.5	−4.2	1.4	−0.2	−0.3	1.00	0.988
3.8	−6.8	−3.3	1.1	−0.1	−0.7	0.99	0.980
5.1	−7.0	−3.9	1.7	−0.05	−0.2	0.99	0.970
10.6	−6.8	−3.4	1.0			1.00	0.939
13.2	−6.9	−3.5	1.2			1.00	0.919
15.2	−7.0	−3.7	1.2			1.00	0.895
$\bar{H}_n$	−7.0±0.2	−3.7±0.3	1.3±0.2	−0.1±0.1	−0.4±0.2		
	Alternate solution with $N2$ and $N3$ reversed						
$\bar{H}_n$	−7.0±0.2	1.1±0.4	−2.3±0.4	0.0±0.2			

we have the best solution and to give an indication of the uniqueness of the solution. This program uses the values obtained in PII and scans cuts in the five-dimensional space of the first five ΔH_n's. This is done, e.g., by scanning ΔH_1 and ΔH_2 while holding ΔH_3 through ΔH_5 at their best PII values, then scanning ΔH_2 and ΔH_3 while holding ΔH_1, ΔH_4, and ΔH_5 at their best PII values, etc. The results of these scans are plotted by the computer as contour plots of the MSD. Figure 4 shows these plots for the outer negative velocity dip of the 5.1 at. % Al alloy. Here we can clearly see many typical features of the analysis. On the ΔH_1 versus ΔH_2 graph we see there are two minimum regions. Since $N1$ and $N2$ have similar weights (8 and 6) there is a reversed solution that is also a fair fit. From the FeSi and FeAl ordered alloys we know the solution with $|\Delta H_1| > |\Delta H_2|$ is the correct solution since the ordered alloys (Fe_3Al type) have only nearest and fourth neighbors and the value obtained for $N1$ in the ordered region agrees with the large value of $|\Delta H_1|$. For many of the analyses there was a definite lower MSD for $|\Delta H_1| > |\Delta H_2|$. Another reversed solution would be that obtained by interchanging the signs of ΔH_2 and ΔH_3. This solution was investigated in detail for the FeAl and FeSi series. For these series ΔH_2 negative and ΔH_3 positive was preferred with the reversed solution being the next minimum on the contour error plots. This reversed solution also had $|H_3| > |H_2|$ and therefore would represent much larger oscillations in the internal field than the regular solution with ΔH_2 negative and larger than ΔH_3. We therefore assume the regular solution is correct although we will quote the values obtained for the reversed solution for the FeAl series in Table II. The ellipticity of the contours on all the graphs is directly related to the number of atoms in a shell, e.g., the contours of ΔH_4 versus ΔH_5 are narrow in the ΔH_4 direction and wide in the ΔH_5 direction, reflecting that $N4$ has 24 atoms and should thus inherently be determined more accurately than $N5$ which has 8 atoms in its shell.

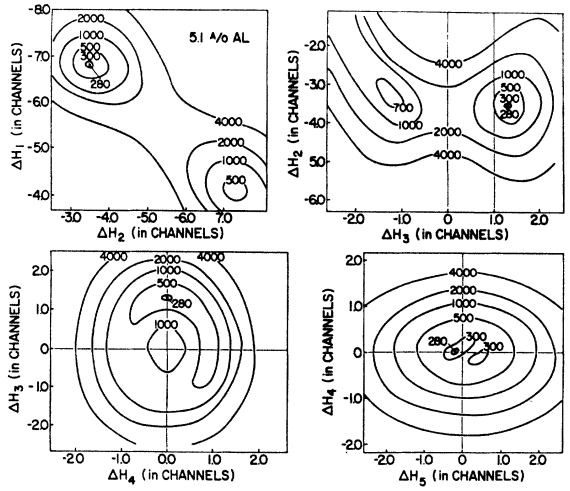

FIG. 4. Contour plots of the mean-square deviation (MSD) of the negative velocity outer line of the 5.1% Al alloy. The scales correspond directly to channels of the multichannel analyzer. In all cases the minimum MSD (280) is shown inside an error contour of 300 (in arbitrary units).

A fourth program (PIV) was used for some of the alloys. This program used the raw data (no pairwise averaging) of the entire spectrum and found the MSD by varying the shifts of the first three neighbors. It is a generalized program of that used to fit the Fe spectra [Eq. (1)] but here the widths Γ_i and powers n_i are not parameters but obtained from the Fe spectra. The ΔH_n values obtained with this program agreed very well with those obtained with PII. The purpose of this program was to test whether using the entire spectrum would give the same results as using just the outer lines and also to see if there appeared to be any quadrupole fields. Figure 5 shows a typical output curve of this program. In all cases tested the internal field shifts with PIV agreed very well with those obtained with PI or PII and there seemed to be no quadrupole fields detectable in any of these alloys.

IV. REMARKS ABOUT RELIABILITY AND CORRECTIONS

For each type of solute atom we ran a whole set of different composition alloys. As the solute-atom content varies, the Mössbauer pattern obtained changes greatly. Figure 3 shows the outer lines of the pure Fe line and a number of different compositions to indicate some typical shapes. As mentioned earlier, since the Fe^{57} excited state has a large natural linewidth, Mössbauer-type experiments have poor resolution (~16 kG) as

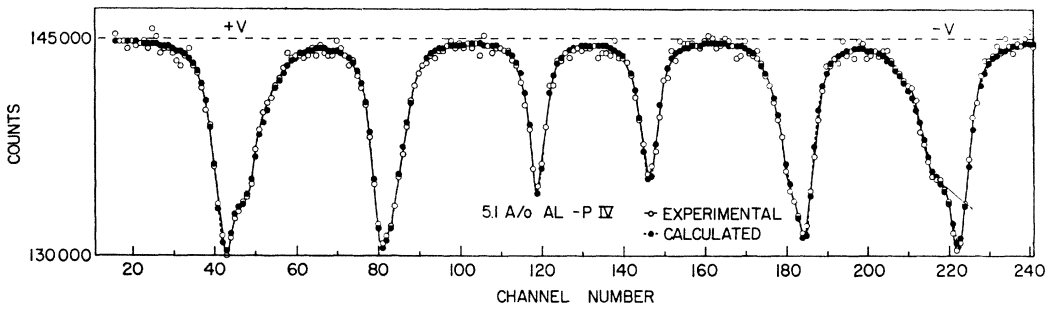

FIG. 5. Comparison of the entire spectrum of the 5.1% Al alloy with the spectrum calculated by computer program PIV. The internal field shifts are the same as those obtained with PII and there is no detectable quadrupole field present. Where the experimental and calculated points are the same, only the former is shown.

compared to ~1 kG for a NMR experiment.[6] In a sense this is helpful since effects such as dipolar broadening due to no longer having cubic symmetry in the alloys and deviations from additivity which would probably be observable with high resolution are not bothersome. It is obvious in looking at the lines obtained (Fig. 3) that we cannot see the individual components by eye. The question arises as to how reliably one can resolve the individual lines with a computer. It appears that if one has the correct model and gets *consistent* results with enough checks and variations built into the programs, one has a necessary but not sufficient condition that the results are reliable. The FeAl and FeSi systems gave particularly consistent results, i.e., the same ΔH 's were obtained for each shell over wide ranges of compositions (and thus for very differently shaped curves). This we feel gives strong evidence that the model is correct and the analysis reliable. If wrong assumptions are made in the analysis or if any unknown effects are being overlooked, we would expect these to be evident in systematic variations of the ΔH_n values as a function of composition. For example, if some unknown effect were causing a broadening of a given type neighbor in such a way that at a given composition it might be mistaken for the effect of a higher shell, then at a different composition the relative weighting of the two shells will be quite different and the shift obtained from the unknown effect would be different from the value at the lower composition.

In analyzing the data we considered two specific types of corrections to the shapes. The first was broadening due to area saturation which arises because of the finite thickness of the absorbers. This effect is present mainly in the more dilute alloys. Thus for alloys of less than 3.5% this correction was made by multiplying the probabilities of configurations containing no $N1$ solute atoms by 0.8 and the probabilities of configurations with no $N2$ solute atoms by 0.9. These factors were suggested from the area ratios which were measured in the pure Fe runs. The changes in the values of ΔH_i's obtained with this correction as compared to the ΔH_i's without the correction were as expected. The values of ΔH_1 and ΔH_3 are essentially unaffected while the value of ΔH_2 was affected in a predictable manner. The reason for this is that ΔH_2 turns out to be intermediate in value between ΔH_1 and ΔH_3 (except for Cr and V) and therefore whereas the components mainly due to $N1$ and $N3$ are on the outer wings of the line shapes those mainly arising from the $N2$ shell are more in the center. This results in ΔH_1 and ΔH_3 being much less sensitivive to the parameters (width and area saturation corrections) used in the analysis. Also since ΔH_1 has a large value, it is particularly insensitive to the parameters, ΔH_3 is smaller and thus more sensitive but not nearly as much as ΔH_2. Thus ΔH_2 is the least reliably determined shift, the parameters used were probably always such as to not overestimate the corrections which would lead to an overestimate for the magnitude of ΔH_2. We estimate that the quoted values of $H_2(=\Delta H_2/H_{Fe}\times 100)$ might be of the order of 1% too large. H_1 and H_3 should be within the accuracy given by their rms errors. The second type broadening is that due to the dipole field from the lack of cubic symmetry in the alloys.[12] Since the polycrystals of the absorber will for the most part be magnetized along the easy direction of magnetization for Fe (100) and all nearest neighbors have $\cos\vartheta=1/\sqrt{3}$, there will be no dipolar broadening of the nearest-neighbor terms. The $N2$ terms have the largest dipole broadening. This can be estimated and gives rise to about a 2% increase in the linewidth. This has a negligible effect. However for NMR experiments this becomes a very important correction and essentially determines the shapes of the satellites.

V. EXPERIMENTAL RESULTS

Some of the data presented here have been previously reported as preliminary work.[1(c)] They have all been reprocessed with the computer programs described above.

FeAl

It appears that of the systems measured, Al solute atoms best fulfill the conditions necessary to interpret

[12] T. E. Cranshaw, C. E. Johnson, and M. S. Radout, in *Proceedings of the International Conference on Magnetism, Nottingham, 1964* (Institute of Physics and the Physical Society, London, 1965).

the results as a measure of the s-conduction-electron polarization in pure Fe. These conditions are that the solute atoms go into the lattice without perturbing the original band structure of the Fe lattice and without any magnetic contribution of their own, that is, we want the solute atom to resemble a hole in the Fe lattice. We can obtain an estimate of the sensitivity of the measurements to each neighbor shell from Table I which gives the ratios of the minimum MSD for successive analysis of the data. We see that ΔH_1, ΔH_2, and ΔH_3 are determined with good sensitivity. ΔH_4 and ΔH_5 are strongly required to be small but we do not have great sensitivity to their particular values. Table II gives the relative percent internal field shifts, $H_n = \Delta H_n/H_{\mathrm{Fe}} \times 100$, for each alloy. Also given is the ratio of the field of Fe atoms containing no Al atoms within the first three to five shells H_0 compared to the field in pure Fe. Note that this field is essentially the same as that in pure Fe for all these alloys. Also quoted are the average relative percent internal field shift $\bar{H}_n$ of each neighbor site and its rms error. The rms error was obtained in the usual way from the deviations of the individual measurements from the average value and contains no estimate of possible systematic errors. As can be seen in Table II, the internal field shifts are independent of Al content. Such independence with concentration supports the assumptions that the Al atoms behave in an isotropic, well-localized manner. This fact combined with the results of many other experiments strongly supports the interpretation that the core polarization remains constant in this alloy system and thus the observed shifts in hyperfine field are due primarily to the indirect exchange interaction of the absent Fe magnetic ion ($S \simeq 1$) with the neighbor Fe^{57} nuclei through the $4s$ conduction band. The other experiments which support this interpretation are: (1) At low Al concentrations (<10 at.%) saturation magnetization measurements[13] show behavior which is well represented by simple dilution, i.e., the moment on the Fe atoms remains unchanged in the Al alloys. Neutron scattering experiments on Fe_3Al have shown that there is no moment on the Al atoms in this ordered alloy.[14] (2) Recent neutron scattering experiments[15] indicate that the magnetic form factor of Fe is not changed for small Al content alloys. Since we expect the core polarization at a Fe^{57} nucleus to be mainly determined by the moment on that atom, (1) and (2) give further evidence that the core polarization remains constant[16] in this series. (3) Heat-capacity measurements by Beck and his coworkers[17] indicate that the density of states at the Fermi surface for the $3d$ electrons remains essentially unaltered upon additions of Al. A similar conclusion has been reached by Van Ostenburg *et al.*[18] from NMR measurements on Al in the V-Al system. Although we have described the electronic states in "localized" language, we do not mean to imply that this type description is necessary. At present magnetism in transition metals is often described by two apparently contradictory models, the localized atomic-like or the diffuse band-type model. It appears to be very difficult to obtain experimental evidence which clearly discriminates between the two models and most experiments can be equally well described in the language of either model.

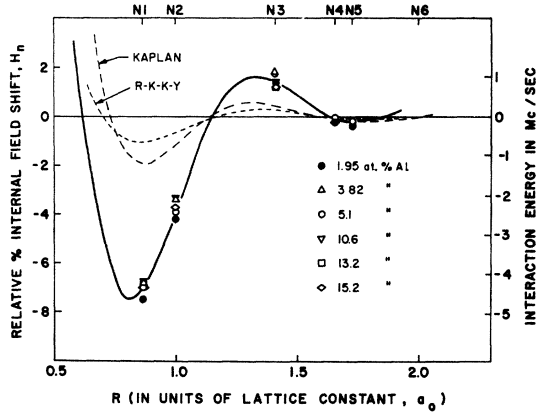

FIG. 6. Relative percent shifts of the internal magnetic field measured at an Fe^{57} atom as caused by putting Al atoms in various neighbor shells. This is identified with the spatial variation of the $4s$ conduction electron spin polarization. The solid curve is calculated from Eq. (10) using a $\chi(q)$ adjusted to give a good fit. (See Ref. 30.) The dotted curve is obtained from RKKY theory and corresponds to a k_F which is a factor 1.25 greater than that of the solid curve. The dashed curve is RKKY theory as corrected by Kaplan (See Ref. 8) to include the k dependence of the periodic part of the $4s$ Block functions.

Figure 6 shows a graph of the measured internal field shifts, or as we shall interpret them, the variation of the $4s$ conduction electron polarization as a function of distance from an iron atom. The comparison of this variation with theory is made in Sec. VI. As mentioned in Sec. III, the data analysis yields other possible sets of H_n's obtained by interchanging sets of neighbors. The next best set after that already given has ΔH_2 and ΔH_3 values nearly interchanged. This second set is also listed in Table II. It has slightly higher MSD values

[13] M. Fallot, Ann. Phys. (Paris), **6**, 305 (1936); A. Arrott and H. Sato, Phys. Rev. **114**, 1420 (1959).

[14] R. Nathans, M. T. Pigott, and C. G. Shull, J. Phys. Chem. Solids **6**, 38 (1958).

[15] A. Arrott, M. F. Collins, T. M. Holden, G. G. Low, and R. Nathans, J. Appl. Phys. Suppl. **37**, 1194 (1966).

[16] Further indication of this type behavior is seen in recent measurements of R. L. Streever and G. A. Uriano [Phys. Rev. **139**, A135 (1965)] on the alloy system of Co in Ni. Using spin-echo techniques they obtained the hyperfine spectra for both the Co^{59} and Ni^{61} nuclei. The magnitude of the shifts and the relative shapes of the spectra were essentially the same for either nucleus showing that both type nuclei felt the same change in internal field for the same occupational configuration. This strongly indicates that the core polarization of both these nuclei remains constant with alloying.

[17] N. Pessall, K. P. Gupta, C. H. Cheng, and P. A. Beck, J. Phys. Chem. Solids **25**, 993 (1964); C. H. Cheng, K. P. Gupta, C. T. Wei, and P. A. Beck, *ibid.* **25**, 759 (1964); K. P. Gupta, C. H. Cheng, and P. A. Beck, *ibid.* **25**, 1147 (1964).

[18] D. O. Van Ostenburg, D. J. Lam, H. D. Trapp, D. W. Pracht, and T. J. Rowland, Phys. Rev. **135**, A455 (1964).

than the first set and is not believed to be a reasonable solution. It would indicate much greater polarizations of the 4s conduction band than obtained from the first set.

It is of some interest to compare these data with the average moment per Fe atom, $\bar{\mu}$ obtained from saturation magnetization measurements. No quantity measured here is exactly equivalent to $\bar{\mu}$, however the most closely related quantity is the average internal field. It is obtained by summing over all possible occupational configurations and is given by

$$\bar{H}_{\text{int}}=H_0-\sum_{n=1}^{5} H_n[\sum_{m_n} m_n p_n(m_n)]. \quad (4)$$

$\bar{H}_{\text{int}}$ is defined relative to the pure Fe field (i.e., $H_{\text{Fe}}=1.0$), $p_n(m_n)$ is the probability of having m_n solute atoms in the nth shell, all other quantities have been previously defined. The last column of Table II lists the $\bar{H}_{\text{int}}$ values and Fig. 7 shows a plot of $\bar{H}_{\text{int}}$ as a function of composition. Also shown are Fallot's[13] measurement of $\bar{\mu}(\mu_{\text{Fe}}=1)$ assuming that all the moment is on the Fe atoms as has been found in neutron scattering experiments.[14] As can be seen the two curves differ, confirming that the quantities measured by the two types of experiments are not identical, one main difference being that the saturation-magnetization measurements are essentially a dc average of the moments whereas the Mössbauer measurements are an average over a nuclear precession time, of the order of 10^{-8} sec. It should be mentioned here that $\bar{H}_{\text{int}}$ is rather insensitive to the model assumed, as long as one obtains good fits to the data, since essentially it represents a centroid of the lines of the spectra and the solutions to different models adjust their values to give essentially the same value for the centroid no matter what model is assumed in the analysis. Thus the values of $\bar{H}_{\text{int}}$ are quite independent of the assumptions which go into the analysis.

The isomer shifts of the first three neighbor shells exhibited the same type additivity as did the internal field shifts. Table VIII lists the isomer shifts caused by the various solute atoms in each of the first three shells. The shifts quoted are relative to an Fe atom in a pure Fe lattice. For example, the shift due to a single Al atom in the first shell is $+0.03\pm0.01$ mm/sec. The average shifts for Al are quite small and indicate a decreased electron density at the Fe nucleus. Within experimental error they are the same for the first three neighbor shells in the Al alloys.

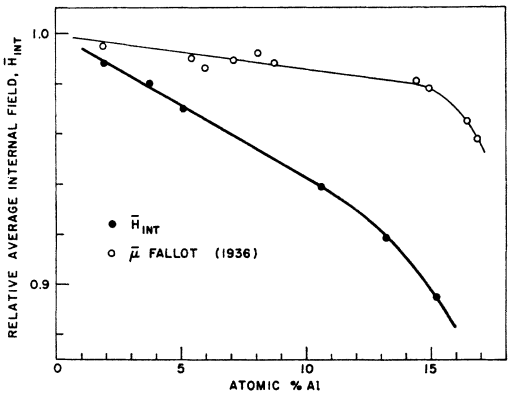

FIG. 7. Average internal magnetic field of FeAl alloys as a function of atomic percent Al. Fallot's 250°K values of the moment per iron atom from saturation-magnetization measurement relative to pure Fe are shown for comparison.

FeSi

The Si alloys are very similar in behavior to the FeAl alloys. Saturation-magnetization measurements[13] at low solute-atom concentrations <6%, show simple dilution and heat-capacity measurements[17] of FeSi alloys have behavior similar to the FeAl alloys. The neutron-scattering experiments[15] which showed no change in the form factor of Fe in alloys with small additions of Al showed a slightly changed form factor with small additions of Si. This may be reflected in the slight differences in behavior of the Si alloys from the Al alloys. The Si atoms, while being quite hole-like in the Fe lattice, may not be as good holes as the Al atoms.

As mentioned earlier, the Si alloys are difficult if not impossible to disorder completely. This manifests itself in the Mössbauer spectra by more prominent bumps in the outer lines than would be expected from the calculated curves. These bumps were heat-treatment-sensitive; they were more pronounced the slower the alloy was cooled. To test whether this ordering affected the analysis strongly we prepared two alloy series, one in which the alloys were cooled only moderately fast and one in which the samples were dropped directly from a temperature of 900°C into a room-temperature oil bath. The latter series had the less pronounced bumps. The internal field shifts obtained for both series were essentially the same, indicating that small amounts of order did not affect the results. We used alloys up to only 5.6% Si, above this percentage there was too much ordering for reliable analysis. Table III gives the ratios of the minimum MSD for successive analysis of this series. As for the Al alloys we have high sensitivity to the first three neighbor shells. ΔH_4 and ΔH_5 are required to be small and have slight sensitivity, and since the alloys are slightly ordered, we do not

TABLE III. Ratios of minimum mean-square deviation for successive analysis of FeSi alloys.

	$N1/N2$		$N2/N3$	
At.% Si	$+v$	$-v$	$+v$	$-\sqrt{2}$
1.8	4.6	3.9	1.3	4.9
2.8	5.5	5.2	1.6	2.2
4.3	6.6	5.0	5.4	2.0
4.8	4.8	4.1	4.6	10.6
5.6	6.2	5.1	5.3	1.1

TABLE IV. Relative percent internal-field shifts and average field for the FeSi series.

At.% Si	H_1	H_2	H_3	H_4	H_0	$\bar{H}_{int}$
1.8	−8.0	−3.5	+1.5		1.00	0.990
2.8	−7.6	−2.7	+1.6		1.00	0.984
4.3	−8.0	−4.1	+1.4	<-0.7	1.01	0.970
4.8	−8.4	−4.8	+2.2	$<+0.7$	0.99	0.972
5.6	−7.9	−4.5	+2.8		1.00	0.970
$\bar{H}_n \pm$rms error	−8.0±0.3	−3.8±0.7	1.9±0.5	0.0±0.7		

quote their values. Table IV gives the relative percent internal field shifts and the relative field H_0 of the Fe atoms surrounded by only Fe atoms in the first three shells. As for the Al alloys this field is nearly the same as the pure Fe field. The field shifts of this series have a behavior very similar to those of the Al series, however here the oscillations appear to be slightly stronger. Figure 8 shows the internal field shifts caused by the Si atoms as a function of the distance between the Si and the Fe atoms. The curve through the data is shown just to indicate the trend of the data. The average isomer shifts for Si alloys are listed in Table VIII. The shifts of Si atoms in the first and second-neighbor shells are slightly greater than those due to Al atoms. There may be a trend to more negative values with distance of the shells. The errors quoted are the rms errors with respect to the average of the whole series.

The average internal field for each alloy was obtained with the use of Eq. (4) and the values are given in the last column in Table IV. Figure 9 shows $\bar{H}_{int}$ plotted as a function of Si content. Shown also are Fallot's[13] room-temperature data of the relative average magnetic moment of Fe obtained from saturation magnetization measurements where it is assumed that the entire moment is on the Fe atoms. As for the Al series, we see that the average internal field decreases more rapidly than the Fe moment. A comparison of $\bar{H}_{int}$ and $\bar{\mu}_{Fe}$ through the ordered alloys (to 26% Si) was given in Ref. 1. As mentioned earlier, since the quantities measured by the two type experiments are different, we do not expect the curves to coincide.

FeMn

The Mn alloys are quite similar in behavior to the Al and Si alloys. The difficulties in preparing these alloys were discussed in Sec. II. After proper precautions they appeared to be very well randomized to about 7% Mn and we could obtain excellent fits to the data. The behavior of the minimum MSD for the successive analysis is similar to that of the Al and Si series for all the alloy series and will no longer be given. Table V

TABLE V. Relative percent internal field shifts and average field for the FeMn series.

At.% Mn	H_1	H_2	H_3	H_4	H_5	H_0	$\bar{H}_{int}$
1.0	−7.5	−5.0	+3.1			1.00	0.995
2.8	−7.6	−3.8	+1.9			1.00	0.983
4.7	−7.9	−4.1	+1.2	−0.4	−1.0	1.01	0.958
6.7	−7.2	−2.2	+0.9	−0.7	−0.75	1.01	0.945

gives the relative internal-field shifts and the ratio of the outer "Fe" lines, H_0, to the pure Fe field. As for the Al and Si series, the Fe atoms with no Mn atoms in the first three to five shells felt essentially the pure Fe field. Figure 10 shows the hyperfine field shifts plotted as a function of distance of the Fe^{57} atom from the solute atom. We see that although the observed behavior is

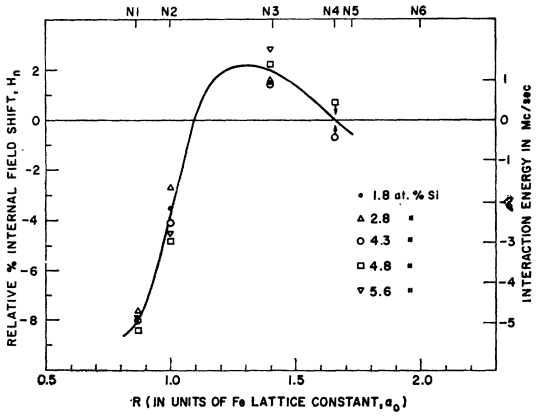

FIG. 8. Relative percent shifts of the hyperfine fields in FeSi alloys as a function of distance from the solute atom. The curve is drawn through the experimental points.

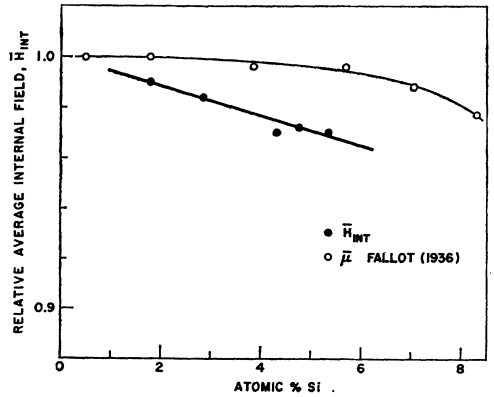

FIG. 9. Average internal magnetic field of FeSi alloys as a function of atomic percent Si. Fallot's room-temperature values of the moment per iron atom from saturation-magnetization measurements are shown for comparison.

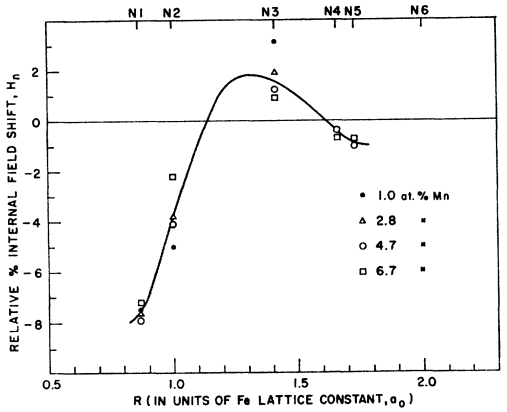

FIG. 10. Relative percent shifts in the internal magnetic field at an Fe^{57} nucleus caused by Mn atoms in FeMn alloys as a function of distance of the Fe atom from the solute atom.

similar to that of Al and Si, the results are not as consistent as for Al and Si. This may be due to a breakdown of the assumptions that go into the analysis since we would expect that Mn atoms would not act like good holes in the iron lattice but would tend to contribute some magnetic behavior.

Figure 11 shows the average internal field as calculated from Eq. (4). Also shown there is the saturation-magnetization data of Sadron and of Arrott and Noakes[19] for dilute alloys of 2 at.% and less. The saturation-magnetization measurements fall slightly above simple dilution. Thus $\bar{H}_{\text{int}}$ appears to fall off faster than the Fe moment as it did for the Al and Si series.

Table VIII lists the average isomer shifts caused by Mn atoms in the first three neighbor shells. We see that the Mn atoms cause no detectable isomer shifts.

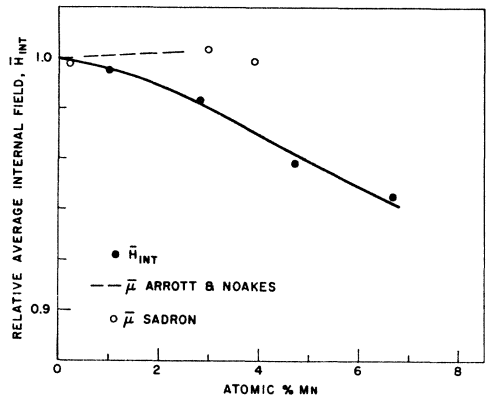

FIG. 11. Average internal magnetic field of FeMn alloys as a function of atomic percent Mn. Shown for comparison are the moments per iron atom from saturation-magnetization measurements.

[19] C. Sadron, Ann. Phys. (Paris) **17**, 37 (1932); A. Arrott and J. E. Noakes, *Iron and Its Dilute Alloys* (John Wiley & Sons, Inc., New York, 1963), p. 93.

FeCr

These alloys tended to order in a manner similar to the Si alloy system showing the least structure when they were rapidly quenched in a hydrogen atmosphere. The fits obtained in the analysis were never as good as for the Al, Si, and Mn series. Alloys of greater than 5.7% Cr could not be fit at all well, part of this may be due to the ordering of the alloys and part may be due to the breakdown in this system of some of the assumptions made in the analysis. Table VI gives the internal field shifts and field H_0 of the Fe atoms surrounded by only other Fe atoms in the first four shells. This field, H_0, is shown in Fig. 13 and is seen to increase with Cr content, that is, all the Fe atoms in the host lattice are affected by adding Cr indicating a nonlocalized behavior. Figure 12 shows a graph of the internal field shifts due to the various neighbors as a function of neighbor distance. In the analysis H_2 definitely preferred to be larger than H_1. The next best solution had H_3 positive, however, the shown solution with H_3 negative seemed to be quite strongly preferred. The curve shown is drawn through the data only to clearly indicate the behavior of the data. As seen in Fig. 12 the behavior of this system is very different from the three previously discussed alloy systems. We would not expect Cr solute atoms to behave like holes in the Fe lattice. We know from many other types of measurements that they contribute to the magnetic behavior in their alloys and

TABLE VI. Relative percent internal field shifts and average field for the FeCr alloys.

At.% Cr	H_1	H_2	H_3	H_4	H_0	$\bar{H}_{\text{int}}$
2.0	−8.6	−9.6	−2.8	−0.2	1.02	0.986
3.7	−8.5	−9.5	−2.65	−0.0	1.03	0.971
5.7	−8.3	−10.8	−1.8	−0.6	1.045	0.949

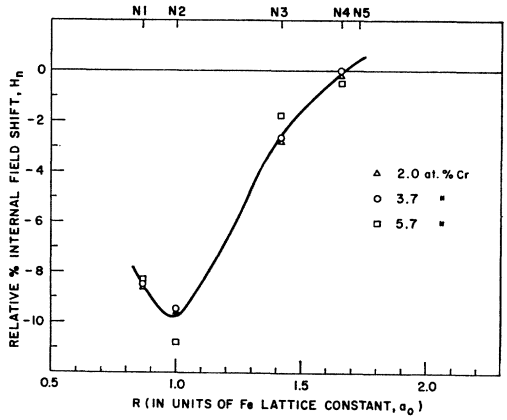

FIG. 12. Relative percent shifts in the internal magnetic field at an Fe^{57} nucleus caused by Cr atoms in FeCr alloys as a function of distance of the Fe atom from the solute atom.

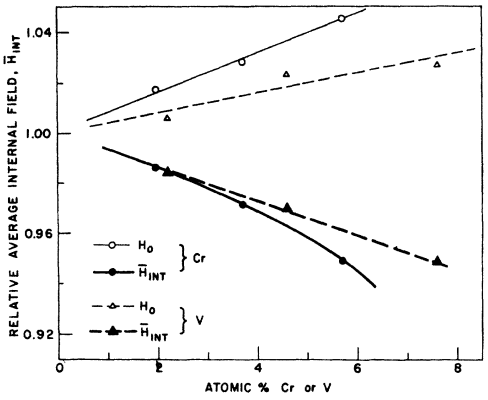

FIG. 13. Average internal magnetic field of FeCr and FeV alloys as a function of percent Cr or V. Also shown is the internal field H_0 of Fe atoms surrounded only by other Fe atoms in the first five neighbor shells.

neutron scattering experiments[15,20] have also indicated that the magnetic disturbance of Cr and V atoms is widespread. Thus this system is not good for measuring the polarization of the conduction electrons in the Fe lattice but it does allow us to see the effects of putting nonlocalized impurities with their own magnetic structure into an Fe lattice. This will be discussed further in Sec. VI.

Table VI lists and Fig. 13 shows the average internal field $\bar{H}_{\text{int}}$ as calculated from Eq. (4) as a function of Cr content. Neutron diffraction studies by Shull and Wilkinson[21] combined with the saturation magnetization data of Fallot[13] give two alternative solutions to the moments on the Fe and Cr atoms in FeCr alloys. The more likely solution is that the Fe moment is nearly constant and equal to that of pure Fe while the Cr moment is opposite to and about one-half that of Fe for concentrations of less than 10% Cr. Thus the moment per Fe atom is probably essentially that of pure Fe over the concentration range measured here. The discrepancy between the average internal field $\bar{H}_{\text{int}}$ and moment per Fe atom, $\bar{\mu}$, for the Cr series is therefore similar to those for the Al and Si series.

Table VIII contains the average isomer shifts caused by Cr atoms in the first three neighbor shells. They are small and slightly negative corresponding to an increase in the charge density at the nearby Fe atoms.

FeV

The behavior of these alloys is similar to the Cr alloys. They tended to order and showed the least structure when rapidly quenched in a hydrogen atmosphere. Fairly good fits were made through the 7.6% alloy. Table VII gives the internal field shifts and field H_0 of the Fe atoms with no solute atoms in the first four shells.

TABLE VII. Relative percent hyperfine field shifts and average field for the FeV alloys.

At.% V	H_1	H_2	H_3	H_4	H_0	$\bar{H}_{\text{int}}$
2.2	−7.5	−7.8	+1.6	−0.4	1.01	0.984
4.6	−8.0	−6.9	+1.1	−0.9	1.02	0.970
7.6	−8.7	−6.2	+1.3	−0.2	1.03	0.949

H_0 is seen to increase with V content and is shown in Fig. 13. Figure 14 shows the internal field shifts plotted as a function of distance of the impurity atom from the measured Fe atom. The solution with $N3$ negative (similar to Cr) was almost as good as the one shown, this one being slightly perferred. The curve through the points is shown just to indicate the trend of the data.

The average internal field $\bar{H}_{\text{int}}$, as calculated from Eq. (4), is given in Table VII and shown plotted as a function of V content in Fig. 13. As seen it decreases slightly less rapidly than the same quantity for Cr. The saturation magnetization data for the FeV system[13,22] are nearly the same as those for FeCr below 10 at.%. Neutron scattering measurements similar to those on the FeCr system have not been made on the FeV system so we do not know how the Fe moment varies with V content. However, since the Cr and V alloys are so similar in many other aspects, it is probable that the Fe moments remain fairly constant below 10% and the discrepancy between $\bar{\mu}$ and $\bar{H}_{\text{int}}$ is similar to all the other alloy systems measured here.

The average isomer shifts for solute atoms in the first three shells are listed in Table VIII. They are small and negative for the first two shells and perhaps positive for the third neighbors, however, since the system may have some ordering, this third value may not be

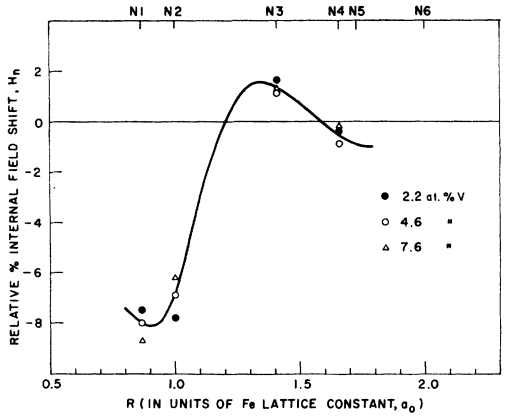

FIG. 14. Relative percent shifts in the internal magnetic field of Fe^{57} atoms caused by V atoms in FeV alloys as a function of distance of the Fe atom from the V atom.

[20] M. F. Collins and G. G. Low, Proc. Phys. Soc. (London) **86**, 535 (1965).
[21] C. G. Shull and M. K. Wilkinson, Phys. Rev. **97**, 304 (1955).
[22] M. V. Nevitt and A. T. Aldred [J. Appl. Phys. **34**, 463 (1963)] have made recent saturation magnetization measurements on the FeV system which are in very good agreement with Fallot's up to about 10 at.% V.

TABLE VIII. Average isomer shifts relative to Fe in Fe(in mm/sec). The errors shown are rms errors.

Series	ΔI_1	ΔI_2	ΔI_3
Al	+0.03±0.01	+0.015±0.01	+0.03±0.02
Si	+0.04±0.02	+0.02 ±0.02	−0.01±0.02
Mn	0.00±0.02	−0.01 ±0.02	0.00±0.02
Cr	−0.01±0.01	−0.05 ±0.03	−0.01±0.02
V	−0.02±0.01	−0.01 ±0.01	+0.02±0.02

meaningful. There may be a trend toward more positive values with distance of the shells.

VI. COMPARISON WITH THEORY

Calculations made in recent years[23] indicate that the direct overlap of the localized $3d$ orbitals does not lower the energy and thus is not responsible for ferromagnetism. Another theoretical approach is that of a "collective" or "itinerant" electron model[24] which starts from the energy band-molecular orbital formalism. However, there are great difficulties associated with obtaining quantitative predictions from these calculations and thus no comparison can be made with experiments. An approach which does give quantitative predictions is that ferromagnetism is caused by the indirect exchange interaction of the coupling of the spins of the magnetic ions via the conduction electrons. Zener[25] originally considered only the static contribution of the conduction electrons to the magnetization while a number of other authors[7] made more complete second-order perturbation calculations which included the off-diagonal matrix elements. These give the familiar oscillatory behavior of the interaction energy as a function of distance from a magnetic ion. The usual RKKY theories give the polarization of the conduction electrons due to the s-d exchange interaction, $\rho(R)$ in the form

$$\rho(R)=\text{const}\int_{k_F}^{\infty}d\mathbf{k}'\int_0^{k_F}d\mathbf{k}\frac{u_{\mathbf{k}}^*(0)u_{\mathbf{k}'}(0)}{E(\mathbf{k})-E(\mathbf{k}')}J(\mathbf{k},\mathbf{k}')\times[e^{i(\mathbf{k}-\mathbf{k}')\cdot\mathbf{R}}-e^{-i(\mathbf{k}-\mathbf{k}')\cdot\mathbf{R}}],\quad(5)$$

where R is the distance from a magnetic ion which is considered at the origin, $\mathbf{k}$ and $\mathbf{k}'$ are the wave vectors of the $4s$ conduction electrons, k_F is the Fermi wave vector, $u_{\mathbf{k}}(0)$ is the periodic part of the Block function $\varphi_{\mathbf{k}}$ evaluated at the origin, and $J(\mathbf{k},\mathbf{k}')$ is the exchange integral between the conduction electrons and the local moment of the magnetic ion. It is given by

$$J(\mathbf{k},\mathbf{k}')\equiv\frac{1}{2S}\sum_i\int d\mathbf{r}_1\times\int d\mathbf{r}_2\varphi_{\mathbf{k}}^*(\mathbf{r}_1)\varphi_i^*(\mathbf{r}_2)\frac{1}{r_{12}}\varphi_{\mathbf{k}'}(\mathbf{r}_2)\varphi_i(\mathbf{r}_1),\quad(6)$$

where the sum is over all localized d orbitals, φ_i, whose spin is S. In early evaluations[7] of $\rho(R)$ a number of simplifying assumptions of questionable validity were made. Some of these are:

(I) The conduction electrons are noninteracting, i.e., $\varphi_{\mathbf{k}}(\mathbf{r})=u_{\mathbf{k}}(\mathbf{r})e^{i\mathbf{k}\cdot\mathbf{r}}$, where $u_{\mathbf{k}}(0)=$ constant.

(II) The spatial distributions of the magnetic ions are represented by δ functions.

(III) Effective mass theory is assumed, i.e., $E(k)\simeq\hbar^2k^2/2m^*$.

(IV) The matrix elements are assumed to be de- on only $q=|\mathbf{k}-\mathbf{k}'|$ rather than on $\mathbf{k}$ and $\mathbf{k}'$.

When all these assumptions are incorporated into (5) and (6), J becomes a constant and we get the original RKKY result,

$$\rho(R)=\text{const}\int\chi_0(q)\cos\mathbf{q}\cdot\mathbf{R}d^3q,\quad(7)$$

where $\chi_0(q)$ is the spin susceptibility function of a non-interacting gas and is given by

$$\chi_0(q)=\chi_p\{\tfrac{1}{2}+[(1-x^2)/4x]\ln(|1+x|/|1-x|)\},\quad(8)$$

where $x=q/2k_F$ and χ_p is the Pauli susceptibility.

We will now proceed to compare (7) and recent improved estimates of (5) with the experimental results. The nature of the internal magnetic field in iron has been discussed by many authors[26] and while not quantitatively satisfactory, it is thought to be quite well understood qualitatively. For Fe it has two main contributions, a minor one $\sim+70$ kG from the unquenched orbital momentum and the major one, which is large and negative due to the Fermi contact interaction. In a cubic material with no spin-orbit coupling this Fermi contact interaction is composed of two parts:

(1) The polarization of the core s electrons due to the exchange interaction with the $3d$ electrons. This is a large negative term.

(2) The polarization of the $4s$ conduction electron which can be considered in two parts:

(a) The polarization of the paired $4s$ conduction electrons due to the exchange interaction with the $3d$

[23] A. J. Freeman and R. E. Watson, Phys. Rev. **124**, 1439 (1961); W. J. Carr, Jr., J. Phys. Soc. Japan **17**, Suppl. B1 (1962).

[24] J. C. Slater, Rev. Mod. Phys. **25**, 199 (1953); E. P. Wohlfarth, *ibid.* **25**, 211 (1953).

[25] C. Zener, Phys. Rev. **81**, 440 (1951); For a discussion of this relative to later work, see J. H. Van Vleck, Rev. Mod. Phys. **34**, 681 (1962).

[26] See, e.g., (a) W. Marshall and C. E. Johnson, J. Phys. Radium **23**, 733 (1962); (b) R. E. Watson and A. J. Freeman, Phys. Rev. **123**, 2027 (1961), *Magnetism* IIA (Academic Press Inc., New York, 1965) p. 167.

electrons; the origin of this term is the same as (1) and gives rise to a positive contribution.

(b) A polarization arising from admixtures of $4s$ electrons with the $3d$ band. This might be quite small due to cancellations.[27]

The total measured internal field is -330 kG [28] and thus it had been concluded that the core electrons are negatively polarized and are mainly responsible for the internal field. Watson and Freeman[26(b)] give an estimate for the $4s$ conduction electron contribution ($2a$) to be $\sim+100$ kG or $+0.3|H_{\mathrm{Fe}}|$.[29] In Sec. V we discussed and concluded that Al solute atoms behave like holes in the Fe lattice and the core polarization at the Fe nuclei remains constant with alloying. We thus assume that for the FeAl system the observed changes in the hyperfine field are due primarily to the indirect exchange interaction of the absent Fe magnetic ion ($S\simeq 1$) with the neighboring Fe^{57} nuclei through the $4s$ conduction electrons. We obtain the value of $\rho(0)$ in the following manner. The net $4s$ polarization in a unit cell is comprised of the sum of the $4s$ spin-density contributions from the cell itself and from all the neighboring cells. The measured internal field contributions arising from the five nearest-neighbor shells are given by the sum of the shifts due to each shell times the number of atoms in the shell; this is $-0.7|H_{\mathrm{Fe}}|$ for Al. Since $\rho(0)$ has to overcome this negative polarization of the surrounding atoms and has a net Fermi contact field, $H_{4s}\simeq+0.3|H_{\mathrm{Fe}}|$, its value is about $+1.0|H_{\mathrm{Fe}}|$. Thus all curves shown in Fig. 6 should be normalized to the ordinate $=100$ at $R=0$.

An initial approach[30] to comparison with theory was to improve assumption (II) by taking the exchange integral $J(q)$ as the magnetic form factor $F_{3d}(q)$. This would be valid in the limit of strong conduction-electron screening of the interelectronic interactions where $1/r_{12}$ could be replaced by a δ function. Then with the framework of still keeping assumptions (I), (III), and (IV), $J(q)$ becomes the magnetic form factor $F_{3d}(q)$ and $\rho(R)$ becomes

$$\rho(R)=\text{const}\int J(q)\chi(q)\cos\mathbf{q}\cdot\mathbf{R}\,d^3q. \tag{9}$$

The original RKKY result, Eq. (7), diverges at the origin so we evaluate Eq. (9) with $\chi(q)=\chi_0(q)$ to obtain an estimate for RKKY theory. The dotted curve of Fig. 6 is the $\rho(R)$ obtained in this way. The Fermi vector k_F is obtained by the scale adjustment in R, and for the curve shown in Fig. 6 is $3.4a_0^{-1}$ or 1.2×10^8 cm^{-1}. This corresponds to about 0.6 electrons/atom in the $4s$ conduction band. The amplitude of the oscillations at the observed R is too small by about a factor of 7. If the curve were renormalized by this factor, it would result in an $H_{4s}\simeq+2000$ kG which is 20 times the estimate for this quantity. Since the agreement with the RKKY theory is unsatisfactory, a further attempt was made to compare Eq. (9) with the experimental results.[30] The spirit of this comparison was to assume Eq. (9) was of the correct form [where $F_{3d}(q)$ was the experimentally measured form factor][31] and to Fourier invert the observed $\rho(R)$ to obtain the form of $\chi(q)$. $\chi(q)$'s were obtained which required a large peak at $2k_F$ and k_F was found equal to 1.0×10^8 cm^{-1} as given in Ref. 30. This approach, however, is premature since the effects of removing some of the other assumptions, (I–IV), should be investigated first. Kaplan[8] recently investigated the effects of assumption (I) by estimating the effect of the k dependence of the periodic part of the $4s$ Block functions. He took $\varphi_{\mathbf{k}}(\mathbf{r})$ to be a single plane wave orthogonalized to the core electrons (hydrogenic wave functions) of the Fe atom. He maintained the "form factor" approximation of $J(q)$ and assumptions (III) and (IV) and obtained a $\rho(R)$ which was essentially unchanged for R values away from the origin and was decreased by a factor 1.8 at $\rho(0)$. This still leaves a factor of about 4 discrepancy with experiment. The dashed curve in Fig. 6 shows the results of theory with this correction included. Kaplan mentions but does not attempt to evaluate a similar type correction which would occur in the exchange integral and thus improve assumption (II). The inclusion of the former correction alone is not sufficient to give good agreement with experiment.

Another recent attempt to improve on the RKKY calculation by removing assumptions (II) and (IV) has been made by Watson and Freeman.[9] They have studied the behavior of $J(\mathbf{k},\mathbf{k}')$ using Gd^{3+} $4f$ wave functions to represent the magnetic-ion spin distribution and plane waves orthogonalized to the Gd core to represent the conduction electrons. They also consider the dependence of J on $\mathbf{k}$ and $\mathbf{k}'$ in their integration processes. They find that J oscillates in sign due to the relative phases of the pair of conduction electron orbitals involved in the exchange integral and the fact that the p-, d-, and f-like components of these orbitals make substantial contributions to the exchange coupling. They then evaluate $\rho(R)$ using their calculated $J(q)$ and the conventional $\chi(q)=\chi_0(q)$ in Eq. (9). They find

[27] P. W. Anderson and A. M. Clogston, Bull. Am. Phys. Soc. **6**, 124 (1961).

[28] S. S. Hanna, J. Heberle, C. Littlejohn, G. J. Perlow, R. S. Preston, and D. H. Vincent, Phys. Rev. Letters **4**, 177 (1960).

[29] T. Muto, S. Kobayasi, and H. Hayakawa, J. Phys. Soc. Japan **20**, 1167 (1965). These authors have made recent calculations which give good agreement with the measured internal field. However to obtain this agreement requires expanding the $3d$ atomic orbitals rather arbitrarily with respect to those of a free atom. They thus obtain a huge core polarization ($\sim-1.2\times10^6$ G) and $4s$ electron exchange polarization ($\sim+700$ kG). These results seem questionable since they lose a striking feature of much of the experimental data, namely, that the observed hyperfine field of Fe^{57} is quite insensitive to its environment, as if the main contributions were from core polarization. [See Ref. 26(b)].

[30] A. W. Overhauser and M. B. Stearns, Phys. Rev. Letters **13**, 316 (1964).

[31] C. G. Shull and Y. Yamada, J. Phys. Soc. Japan **17**, Suppl, BIII, 1 (1962); R. Nathans, S. J. Pickhart, and H. A. Alperin. *ibid.* **17**, Suppl. BIII, 7 (1962).

that $\rho(r)$ can have rather wild oscillatoins at distances less than the nearest-neighbor distances and that $\rho(0)$ can be either positive or negative but most important that the ratio of $\rho(0)/\rho(R_{N1})$ can be small as compared with RKKY theory where this ratio is of the order of 100. These authors have carried out similar calculations for Fe but because of the nature of the Fe wave functions these results are less reliable than the results for Gd.[32] The fact, however that one obtains strong qualitative changes in $\rho(R)$ for the Gd wave functions suggests that similar changes may occur for iron and thus lead to agreement between the improved RKKY theory and the experimental results. However to definitely conclude that the Fe calculations with a conventional $\chi_0(q)$ can be made to agree with the observed oscillations appears to require much more detailed and elaborate calculations incorporating the removal of all three assumptions (I), (III), and (IV). Indications from present calculations are that such agreement may be possible.

We would expect that adding solute atoms with their own magnetic structure would have a large effect on the form of the exchange integral Eq. (6) and thus on the shape of the polarization $\rho(R)$. We indeed observed that the internal-field variation with distance for the FeCr system is quite different from the FeAl system. In principle we should be able to put in the correct magnetic-ion wave function and obtain the different form of $\rho(R)$; however in practice this is quite beyond present computational abilities.

VII. CONCLUSIONS

There seems to be strong experimental evidence that the observed variations in internal fields in the FeAl series (and fairly well in the FeSi series) can be interpreted as a measure of the spin polarization of the 4*s* conduction electrons. Making the usual assumption that the hyperfine field due to the 4*s* electrons is mainly determined directly by their polarization (and not e.g., by their polarization of the core electrons), an outstanding feature of this measured polarization is that the 4*s* electron at the first and second neighbors are polarized opposite to the 3*d* electrons. Thus if the 4*s* conduction electrons played the dominant role in determining magnetism in iron, it would be antiferromagnetic. However, we should not expect these electrons but rather the itinerate *d*'s to be the dominant factor as indicated by this negative polarization. The approximations made in the original form of RKKY theory of *s-d* exchange polarization lead to a large discrepancy between theory and the measurements. However, recent calculations, taking into account the k dependence of the wave functions and spatial extent of the magnetic ions, indicate that it may be possible to bring theory into agreement with experiment.

The average internal magnetic field as a function of the percent of solute atoms for all the alloy series investigated decreases more rapidly than the variation of the magnetic moment per Fe atom.

The isomer shifts are small and of either sign with respect to Fe in an Fe lattice. There appear to be no quadrupole shifts in any of the alloys.

ACKNOWLEDGMENTS

The author is grateful to Dr. A. W. Overhauser for many enlightening discussions on all aspects of this work and S. S. Wilson for invaluable assistance throughout the experiment. Dr. H. Sato and Dr. A. Arrott also gave valuable advice and helpful discussions throughout the course of this work.

[32] R. E. Watson (private communication).